NATIONAL ADVISORY COMMITTEE
FOR AERONAUTICS

TECHNICAL NOTE 4289

BOUNDARY-INDUCED DOWNWASH DUE TO LIFT IN A

TWO-DIMENSIONAL SLOTTED WIND TUNNEL

By S. Katzoff and Raymond L. Barger

Langley Aeronautical Laboratory
Langley Field, Va.

NACA

NATIONAL ADVISORY COMMITTEE FOR AERONAU

TECHNICAL NOTE 4289

BOUNDARY-INDUCED DOWNWASH DUE TO LIFT IN A

TWO-DIMENSIONAL SLOTTED WIND TUNNEL

By S. Katzoff and Raymond L. Barger

SUMMARY

A solution has been obtained for the complete tunnel-interference flow for a lifting vortex in a two-dimensional slotted tunnel. Curves are presented for the longitudinal distribution of tunnel-induced down-wash angle for various values of the boundary openness parameter and for various heights of the vortex above the tunnel center line. Some quantitative discussion is given of the use of these results in calculating the tunnel interference for three-dimensional wings in rectangular tunnels with closed side walls and slotted top and bottom.

INTRODUCTION

The problem of determining lift interference corrections for slotted-throat tunnels by using an approximate "homogeneous" boundary condition has been treated by several authors (refs. 1 to 3). For both two- and three-dimensional tunnels, results have been given for the vertical inter-ference velocity at a lifting vortex located on the tunnel center line. (See, for example, ref. 1.)

This report extends the two-dimensional results of reference 1 by giving the longitudinal distribution of this vertical interference veloc-ity along the horizontal line through the vortex, for various vertical positions of the vortex in the tunnel. The manifest application of these results is to the determination of the tunnel-induced angle of attack and camber in two-dimensional airfoil testing. An important further appli-cation is to the determination of the tunnel-induced downwash angle in three-dimensional-model testing. The feasibility of the latter appli-cation was pointed out in reference 2 and will be further discussed in the present report.

As in the previous tunnel-interference studies, the analysis is made for incompressible flow. For the present problem, which considers only the tunnel-induced vertical velocity for given lift, the compressibility

effect can be taken into account merely by reading the induced angle at $x/\sqrt{1 - M^2}$ instead of at x (Göthert rule).

The method of solution of the problem is considered to be of particular interest. It uses a generalized Fourier series in a form that automatically satisfies the boundary conditions. The method has apparently not been used in previous wind-tunnel interference studies, although similar methods of solution have been used, for example, for problems involving thermal diffusion (ref. 4) and stress diffusion (ref. 5).

<div align="center">SYMBOLS</div>

A_n, B_n constant coefficients in the series expansion for φ

$g = \dfrac{l}{h}$

c chord of two-dimensional airfoil

c_l lift coefficient of two-dimensional airfoil

C area of tunnel cross section

C_L wing lift coefficient

d slot spacing (distance between center lines of slots)

k height of vortex above tunnel center line, expressed as fraction of tunnel semiheight

h tunnel semiheight

l apparent mass associated with flow normal to slotted boundary, per unit area of boundary, $\dfrac{d}{\pi} \log_e \csc \dfrac{\pi\sigma}{2}$

M Mach number

r_n root of equation (2a)

R_n root of equation (2b)

S wing area

V   tunnel free-stream velocity

x, z   rectangular coordinates, expressed as fraction of tunnel
                             semiheight (fig. 1)

Γ vortex strength, positive clockwise (lifting)

δ tunnel correction factor

$\delta_{2\text{-dim}}$ two-dimensional-tunnel correction factor

δ_c that part of the total tunnel correction factor contributed
                             by the center row of images

$\Delta\delta$ error in tunnel correction factor incurred by using two-
                             dimensional vortices in place of the exact images in the
                             rows above and below the center row; defined only for
                             closed tunnels or for tunnels with completely open top
                             and bottom boundaries

ϵ tunnel-induced downwash angle

φ total perturbation potential (due to lifting vortex and
                             tunnel interference)

φ_1 potential of lifting vortex

φ_2 potential of tunnel interference

σ open ratio of slotted boundary (ratio of slot width to
                             slot spacing)

BASIS OF METHOD OF SOLUTION

The boundary condition at a slotted wall, considered as an equiva-
lent homogeneous boundary, is derived in references 1, 2, and 3 as

$$\varphi + l\,\frac{\partial\varphi}{\partial n} = 0$$

where

φ perturbation potential

$\dfrac{\partial \varphi}{\partial n}$ derivative of φ in the direction of the outer normal
                         at the boundary

$l = \dfrac{d}{\pi} \log_e \csc \dfrac{\pi \sigma}{2}$

d   slot spacing

σ open ratio of slotted boundary (ratio of slot width to
                         slot spacing)

For the present problem of the two-dimensional tunnel it will be
convenient to make all lengths nondimensional by dividing by the tunnel
semiheight h; in other words, the tunnel semiheight will be taken as
unity. A sketch of this tunnel showing the coordinate system and the
lifting (bound) vortex is shown in figure 1. The boundary condition
may be written

$$\varphi + g \frac{\partial \varphi}{\partial z} = 0 \qquad\qquad (z = 1) \qquad (1a)$$

$$\varphi - g \frac{\partial \varphi}{\partial z} = 0 \qquad\qquad (z = -1) \qquad (1b)$$

where $g = \dfrac{l}{h}$.

The boundary condition can be automatically satisfied by making
use of a trigonometric Fourier series of a more general form than that
commonly used. Consider the functions $\sin r_n z$ and $\cos R_n z$
$(n = 1, 2, 3, \ldots)$ where the r_n are the positive roots of

$$\tan r + gr = 0 \qquad\qquad\qquad (2a)$$

and the R_n are the positive roots of

$$\cot R - gR = 0 \qquad\qquad\qquad (2b)$$

The functions $\sin r_n z$ and $\cos R_n z$ form a complete orthogonal set over the interval $-1 \leq z \leq 1$ (ref. 4). The series

$$s = \sum_{n=1}^{\infty} A_n \sin r_n z + B_n \cos R_n z$$

satisfies the conditions (1a) and (1b) at $z = 1$ and $z = -1$, respectively, because

$$\left[s + g \frac{\partial s}{\partial z}\right]_{z=1} = \sum_{n=1}^{\infty} A_n\left(\sin r_n + gr_n \cos r_n\right) + B_n\left(\cos R_n - gR_n \sin R_n\right)$$

$$\left[s - g \frac{\partial s}{\partial z}\right]_{z=-1} = \sum_{n=1}^{\infty} A_n\left(-\sin r_n - gr_n \cos r_n\right) + B_n\left(\cos R_n - gR_n \sin R_n\right)$$

where the quantities in parentheses are all zero because of conditions (2a) and (2b). Hence, any series of the form

$$s = \sum_{n=1}^{\infty} A_n f_n(x)\sin r_n z + B_n F_n(x)\cos R_n z$$

representing a function in the xz-plane automatically satisfies the boundary conditions (1a) and (1b).

It is of interest to note that the arguments of the functions of a Fourier-Bessel series can be similarly chosen so that each term satisfies the boundary condition $\varphi + g \frac{\partial \varphi}{\partial n} = 0$ on the boundary of a circle (ref. 6).

APPLICATION TO THE PROBLEM OF THE LIFTING VORTEX

Boundary conditions.- In reference 1 it was shown that the total perturbation flow (vortex flow plus boundary interference) in the tunnel could be considered to have two parts: (1) an antisymmetric part

characterized by a uniform upwash velocity far upstream, an equal uniform
downwash velocity far downstream, and zero downwash along the vertical
axis (the z-axis) through the vortex itself, and (2) a flow with uniform
downwash velocity throughout the entire tunnel, of such magnitude that
it cancels the upstream upwash velocity of part (1) and thereby provides
zero net effect far upstream and uniform downwash velocity along the
z-axis. The value of this uniform downwash velocity (for the tunnel of
unit semiheight) was shown to be $\dfrac{\Gamma}{4(g+1)}$. This value was derived in
reference 1 for the case of the vortex at the origin; however, the line
of reasoning is not altered by changing the vertical location of the
vortex in the tunnel, so that the same expression remains applicable in
the general offcenter case. Accordingly the potential along the z-axis is
given by $-\dfrac{\Gamma z}{4(g+1)} + \dfrac{\Gamma}{4}$ above the vortex location and by $-\dfrac{\Gamma z}{4(g+1)} - \dfrac{\Gamma}{4}$
below the vortex location. (The potential is here considered to increase
in the direction of flow, contrary to the usage in reference 1; also, a
clockwise (lifting) vortex is here considered as positive.)

The problem will be solved for the upstream half of the tunnel:
$x \leqq 0$, $-1 \leqq z \leqq 1$; the solution for the downstream half follows from
the known symmetry characteristics. For the upstream half, then, the
problem, as given by the preceding discussion, is to find an expression
for φ that satisfies Laplace's equation, satisfies equations (1a) and
(1b), approaches zero as x approaches $-\infty$, and along the z-axis equals
$-\dfrac{\Gamma z}{4(g+1)} + \dfrac{\Gamma}{4}$ above the vortex and $-\dfrac{\Gamma z}{4(g+1)} - \dfrac{\Gamma}{4}$ below the vortex.

Solution for total perturbation flow.- The total perturbation
potential is expressed in the form

$$\varphi = \sum_{n=1}^{\infty} A_n e^{r_n x} \sin r_n z + B_n e^{R_n x} \cos R_n z \qquad (3)$$

where the r_n and R_n are the positive roots of equations (2a) and (2b),
respectively. The coefficients A_n and B_n are determined by matching
the expression with the known potential along the z-axis. That is, let

$$\sum_{n=1}^{\infty} A_n \sin r_n z + B_n \cos R_n z = -\frac{\Gamma z}{4(g+1)} + \begin{cases} \dfrac{\Gamma}{4} & (k < z < 1) \\ 0 & (z = k) \\ -\dfrac{\Gamma}{4} & (-1 < z < k) \end{cases}$$

Since the terms of the series are orthogonal in the range $(-1, 1)$, each A_n is found by multiplying both sides of the equation by $\sin r_n z \, dz$ and integrating from -1 to 1:

$$A_n \int_{-1}^{1} \sin^2 r_n z \, dz = -\frac{\Gamma}{4(g+1)} \int_{-1}^{1} z \sin r_n z \, dz - \frac{\Gamma}{4} \int_{-1}^{k} \sin r_n z \, dz + \frac{\Gamma}{4} \int_{k}^{1} \sin r_n z \, dz$$

$$= -\frac{\Gamma}{4(g+1)} \int_{-1}^{1} z \sin r_n z \, dz + \frac{\Gamma}{2} \int_{k}^{1} \sin r_n z \, dz$$

Applying the same procedure to the cosine term gives

$$B_n \int_{-1}^{1} \cos^2 R_n z \, dz = -\frac{\Gamma}{4} \int_{-1}^{k} \cos R_n z \, dz + \frac{\Gamma}{4} \int_{k}^{1} \cos R_n z \, dz$$

$$= -\frac{\Gamma}{2} \int_{0}^{k} \cos R_n z \, dz$$

Performing the indicated integrations and simplifying the results by means of equations (2a) and (2b) yields

$$A_n = \frac{\Gamma}{2r_n} \frac{\cos r_n k}{1 + g \cos^2 r_n}$$

$$B_n = -\frac{\Gamma}{2R_n} \frac{\sin R_n k}{1 + g \sin^2 R_n}$$

Substituting these expressions for the coefficients in equation (3) completely determines φ in the region $x < 0$.

Tunnel-interference velocity.- The potential φ just derived is the sum of the potential $\varphi_1 = -\frac{\Gamma}{2\pi} \tan^{-1} \frac{z-k}{x}$ of the lifting vortex and the potential φ_2 of the tunnel interference: $\varphi = \varphi_1 + \varphi_2$. The desired tunnel-interference upwash velocity $\frac{\partial \varphi_2}{\partial z}$ is found by subtracting $\frac{\partial \varphi_1}{\partial z}$ from $\frac{\partial \varphi}{\partial z}$:

$$\frac{\partial \varphi_2}{\partial z} = \frac{\partial \varphi}{\partial z} - \frac{\partial \varphi_1}{\partial z}$$

$$= \frac{\Gamma}{2} \sum_{n=1}^{\infty} \left(\frac{e^{r_n x} \cos r_n k \cos r_n z}{1 + g \cos^2 r_n} + \frac{e^{R_n x} \sin R_n k \sin R_n z}{1 + g \sin^2 R_n} \right) +$$

$$\frac{\Gamma}{2\pi} \frac{x}{x^2 + (z - k)^2} \qquad\qquad\qquad\qquad (x < 0)$$

The entire model may generally be considered with adequate accuracy to lie in one horizontal plane. Then, since the interference is of interest only in this plane, z may be set equal to k in the preceding equation to give

$$\frac{\partial \varphi_2}{\partial z} = \frac{\Gamma}{2} \sum_{n=1}^{\infty} \left(\frac{e^{r_n x} \cos^2 r_n k}{1 + g \cos^2 r_n} + \frac{e^{R_n x} \sin^2 R_n k}{1 + g \sin^2 R_n} \right) + \frac{\Gamma}{2\pi x} \qquad (x < 0) \qquad (4)$$

Equation (4) gives the tunnel-induced upwash velocity in the upstream part of the tunnel. At $x = 0$, the upwash velocity is $-\dfrac{\Gamma}{4(g + 1)}$, as already mentioned. The tunnel-induced upwash velocity in the downstream part of the tunnel follows from the symmetry characteristics previously described; that is,

$$- \frac{\Gamma}{4(g + 1)} - \frac{\partial \varphi_2}{\partial z}\bigg]_{x, z} = \frac{\partial \varphi_2}{\partial z}\bigg]_{-x, z} - \left[- \frac{\Gamma}{4(g + 1)} \right]$$

or

$$\frac{\partial \varphi_2}{\partial z}\bigg]_{x, z} = - \frac{\Gamma}{2(g + 1)} - \frac{\partial \varphi_2}{\partial z}\bigg]_{-x, z}$$

where the symbol $\bigg]$ means the value of the derivative at the point indicated by the subscript.

Calculated results.- The tunnel-induced vertical velocities were computed for points along the horizontal line through the bound vortex, for ranges of values of g and k that are considered to more than cover the likely ranges of slot designs and airfoil locations. The results are plotted in figure 2 in nondimensional form as $\frac{\epsilon h V}{\Gamma}$, where

ϵ is downwash angle and V is tunnel speed. For direct application to two-dimensional airfoil testing, the equivalent expression in terms of chord c and section lift coefficient c_l, $\frac{2\epsilon h}{c c_l}$, is also shown. The expression corresponds to the usual three-dimensional-tunnel correction factor δ defined by

$$\epsilon = \delta \frac{S}{C} C_L$$

where S is wing area, C is the area of the tunnel cross section, and C_L is the wing lift coefficient.

The two limiting cases - the closed tunnel $(g \doteq \infty)$ and the open tunnel $(g = 0)$ - are not included in figure 2 because closed expressions, readily derived by the method of images, are available for these cases. For the closed tunnel,

$$\delta_{2\text{-dim}} = \frac{1}{8}\left[\frac{\cosh\frac{\pi x}{4}\cos^2\frac{\pi h}{2}}{\sinh\frac{\pi x}{4}\left(\sinh^2\frac{\pi x}{4}+\cos^2\frac{\pi h}{2}\right)} - \frac{1}{\frac{\pi x}{4}}\right]$$

For the open tunnel,

$$\delta_{2\text{-dim}} = \frac{1}{4} + \frac{1}{8}\left[\frac{\cosh\frac{\pi x}{4}}{\sinh\frac{\pi x}{4}}\left(1 + \frac{\sinh^2\frac{\pi x}{4}}{\sinh^2\frac{\pi x}{4}+\cos^2\frac{\pi h}{2}}\right) - \frac{1}{\frac{\pi x}{4}}\right]$$

ESTIMATING CORRECTIONS FOR THREE-DIMENSIONAL MODELS

Suggested correction as the sum of two parts.- In reference 2 it was suggested that two-dimensional results such as those derived in the preceding section could be applied in determining corrections for three-dimensional models in rectangular wind tunnels with closed side walls and slotted upper and lower boundaries, provided the height-width ratio

of the tunnel is not too small. Specifically, the tunnel-induced angle
at any point would be the sum of two parts: (1) that due to the infinite
row of images of the model in the vertical walls, and (2) the two-
dimensional corrections of figure 2, determined as for a two-dimensional
wing of the same lift at the same longitudinal location in the tunnel.
The purpose of the present section is to review the theory of this method
and to provide some quantitative discussion of the method and of the tun-
nel height-width ratios for which it can be considered satisfactory. For
the smaller height-width ratios, for which the method is not quite valid,
a further suggestion is given by which the method might still be used
with an additional modification.

A complete analysis should include comparisons between induced angles
determined by this suggested method and those determined by some exact
method similar, say, to those outlined in reference 1. Such exact three-
dimensional calculations would be very laborious, however, for the case
of the tunnel with slotted upper and lower boundaries. Accordingly, the
present approach will be to make exact calculations for the cases of com-
pletely open and completely closed top and bottom boundaries, which are
the two limiting cases of slotted boundaries, and then to apply arguments
of plausibility in extending the results to the case of slotted boundaries.

Formulation of problem for the two limiting cases.- Figure 3(a)
shows the cross section of a closed rectangular tunnel (heavy outline)
with its nearest images. The plus sign in the center of the tunnel
represents the semi-infinite doublet line (or horseshoe vortex of zero
span) trailing downstream from a point concentration of lift in the cen-
ter of the tunnel. The image doublet lines are indicated by plus or
minus signs according as they are the same as or the reverse of the cen-
ter one. The tunnel-induced downwash or upwash velocity at any point in
the tunnel (say at the lifting element itself or at some downstream point
representing the tail location) is the net induced velocity due to all
the images. The concepts underlying this figure and the application of
this theory have been widely used in wind-tunnel-correction analysis (for
example, refs. 7 and 8) and will not be further discussed here.

As pointed out in references 7 and 8, the field of a doublet line
at a point sufficiently distant from it is practically the same as the
field of a narrow horseshoe vortex having the same moment (same product
of vortex strength and span - in other words, the same lift). Suppose,
then, it were valid to replace all the image doublet lines in the rows
above and below the center row by horseshoe vortices of span equal to
the tunnel width. The trailing vortices would all cancel in pairs and
only the bound vortices, now joined to form continuous infinitely long
vortices, would remain, as indicated in figure 3(b). This set of joined
bound vortices, however, will be recognized as identical with the set of
image bound vortices that are used to calculate corrections for a closed
two-dimensional tunnel (ref. 9). If the image system of figure 3(b) were

indeed an accurate approximation for the image system of figure 3(a), it would follow that the tunnel-induced angle for this case is the sum of (1) the effect of the images in the center row and (2) the two-dimensional correction, just as suggested in the opening paragraph of the preceding section.

The corresponding image diagrams for the tunnel with open top and bottom are shown in figures 4(a) and 4(b). The argument is essentially the same as for the closed tunnel and will not be repeated.

The problem now is to determine for what height-width ratios the image systems of figures 3(b) and 4(b) satisfactorily approximate the exact image systems of figures 3(a) and 4(a), respectively, so that the suggested calculation procedure would be accurate.

Calculations of the error.- In order to investigate this problem, calculations were made of the error in the induced-angle factor δ along the tunnel center line that would result from using the image systems of figures 3(b) and 4(b) instead of those of figures 3(a) and 4(a), respectively. The calculations were made for tunnel height-width ratios of 0.6, 0.75, 1.0, and 1.2. These calculations for the zero-span horseshoe vortices (or point concentrations of lift in the center of the tunnel), however, represent the least favorable case. In order to investigate the problem for conditions more nearly representative of typical wing tests, calculations were also made for horseshoe vortices of span equal to 0.4 the tunnel width. As a somewhat extreme case, some calculations were also made for horseshoe vortices of span equal to 0.8 the tunnel width. For the limiting case, for which the horseshoe vortex has a span equal to the tunnel width, the exact image system would be identical with the two-dimensional image system, and thus the error would be zero for any height-width ratio.

The calculated errors are plotted in figure 5 as the error $\Delta\delta$ in the usual tunnel correction factor δ in the equation

$$\epsilon = \delta \frac{S}{C} C_L$$

Specifically, $\Delta\delta$ is the induced downwash factor given by the exact image system minus the induced downwash factor given by the approximate image system. The approximate image system gives too small a downwash angle (too small a factor) for the open top and bottom and too large a downwash angle (too large a factor) for the closed tunnel. In other words, $\Delta\delta$ is positive for the tunnel with open top and bottom, and is negative for the closed tunnel. The value of $\Delta\delta$ at $x = 0$ represents the error at the lifting element itself; values at positive values of x represent the error in downwash behind the wing. The upstream (negative x)

parts of the curves are not shown, since the curves all have the same type of symmetry as the curves of figure 2.

As an indication of the order of magnitude of the error that might arise, consider the largest value of $\Delta\delta$ in figure 5, 0.092, for the tunnel with a height-width ratio of 0.6. If the wing area S is one-tenth the tunnel cross-sectional area C and the lift coefficient C_L is 1.0; the corresponding error in tunnel-induced angle is $0.092 \times 0.1 \times 1.0 \times 57.3^\circ = 0.53^\circ$. The error decreases rapidly with increasing height-width ratio and with increasing span of the horseshoe vortex, and it is well within usual experimental accuracy for height-width ratios of about 1.0.

Application to the slotted tunnel.- For those tunnel height-width ratios for which the results show no practically significant differences between the field of the true image system and the field of the system of infinite line vortices that approximates it, it would seem reasonable to suppose that the effect of slotted top and bottom boundaries would be similarly two-dimensional. In those cases in which the difference does become practically significant (for example, for tunnel height-width ratios less than 1.0 with the larger lift coefficients and wing areas) the matter is less obvious. A suggested approach is as follows:

Let the curves of figure 5 be considered as correction curves rather than as error curves. That is, suppose that the tunnel-induced angle (for the completely open or completely closed top and bottom) is considered to be the sum of the following three components:

(1) That due to the images in the center row

(2) The two-dimensional induced angles corresponding to the infinite line vortices of figure 3(b) or 4(b)

(3) The correction indicated by figure 5, which, essentially, corrects the two-dimensional values of component (2) to the correct three-dimensional value corresponding to figure 3(a) or 4(a).

Then a parallel procedure for the tunnel with slotted top and bottom would be to suppose the tunnel-induced angle to be the sum of the following three components:

(1) That due to the images in the center row

(2) The two-dimensional induced angles given by figure 2 for the appropriate value of g

(3) A correction determined by interpolating between the closed and open cases of figure 5. The interpolation could be according to

the "degree of openness" of the slotted boundary as indicated, say, by the factor $\frac{1}{g+1}$ that determines the two-dimensional correction at $x = 0$. This factor is zero for the closed tunnel ($g = \infty$) and 1 for the open tunnel ($g = 0$). According to this suggested interpolation procedure, the contribution of this third component to δ is

$$\Delta\delta_{closed} + \frac{1}{g+1}\left(\Delta\delta_{open} - \Delta\delta_{closed}\right)$$

where $\Delta\delta_{closed}$ and $\Delta\delta_{open}$ are the values of $\Delta\delta$ given by figure 5 for the closed and open cases, respectively. Furthermore, since, as figure 5 shows, $\Delta\delta_{open}$ and $\Delta\delta_{closed}$ are almost equal, except for sign, this expression may be approximated as

$$-\Delta\delta_{open} + \frac{2}{g+1}\Delta\delta_{open}$$

or

$$\frac{1-g}{1+g}\Delta\delta_{open}$$

If the slot design is such that $g = 1$, this third component will be approximately zero.

In order to help in the application of this procedure, the first component δ_c, due to the images in the center row, has been plotted in figure 6. The net induced downwash factor, finally, is

$$\delta = \delta_c + \delta_{2\text{-dim}} + \frac{1-g}{1+g}\Delta\delta_{open}$$

where δ_c is given by figure 6, $\delta_{2\text{-dim}}$ is given by figure 2, and $\Delta\delta_{open}$ is given by figure 5 (positive values).

Asymmetric locations of the model in the tunnel.- A sting-mounted model might, at high angles of attack, be considerably above the tunnel center line. Figure 7(a) shows the image system for such an asymmetric case, for a point concentration of lift in a closed tunnel. The corresponding approximation by means of infinite vortices is shown in figure 7(b). No calculations were made for this case, but it is apparent from the image system that the error is very nearly the average of that

for a tunnel whose height is the distance m_1 to the nearer row and that for a tunnel whose height is the distance m_2 to the farther row. Except for this one modification, the discussion for the slotted-boundary tunnel follows as before.

Yawing a sting-mounted model also tends to increase the error. Figure 8(a) shows the image system for an extreme case in which the point concentration of lift has been brought close to one of the side walls. The image system in this case is very nearly the same as for a centered model in a tunnel of half the height-width ratio (fig. 8(b)), for which the error is greatly increased. Fortunately, lateral displacement of the lifting point to the extent shown in figure 8(a) is far in excess of what might be considered a realistic displacement due to yawing a model in a wind tunnel.

CONCLUDING REMARKS

A practical mathematical method is described for determining the flow in a two-dimensional slotted wind tunnel containing a lifting wing. Calculated results are given for the longitudinal distribution of tunnel-induced angles for various slot geometries and for various vertical locations of the wing in the tunnel. Some quantitative discussion is given of the application of these results to the testing of three-dimensional lifting models in a tunnel with closed side walls and slotted top and bottom.

Langley Aeronautical Laboratory,
    National Advisory Committee for Aeronautics,
        Langley Field, Va., March 6, 1958.

REFERENCES

1. Davis, Don D., Jr., and Moore, Dewey: Analytical Study of Blockage-
   and Lift-Interference Corrections for Slotted Tunnels Obtained by
   the Substitution of an Equivalent Homogeneous Boundary for the
   Discrete Slots. NACA RM L53E07b, 1953.

2. Maeder, P. F.: Theoretical Investigation of Subsonic Wall Interference
   in Rectangular Slotted Test Sections. Tech. Rep. WT-11 (Contract AF 18
   (600)-664), Div. Eng., Brown Univ., Sept. 1953.

3. Guderley, Gottfried: Wall Corrections for a Wind Tunnel With Longi-
   tudinal Slots at Subsonic Velocities. WADC Tech. Rep. 54-22,
   Wright Air Dev. Center, U. S. Air Force, Jan. 1954.

4. Byerly, William Elwood: An Elementary Treatise on Fourier's Series and
   Spherical, Cylindrical, and Ellipsoidal Harmonics. Ginn and Co.,
   c.1893.

5. Mansfield, E. H.: The Effect of Spanwise Rib-Boom Stiffness on the
   Stress Distribution Near a Wing Cut-Out. R. & M. No. 2663,
   British A.R.C., Dec. 1947.

6. Watson, G. N.: A Treatise on the Theory of Bessel Functions. Second
   ed., The MacMillan Co., 1944, ch. XVIII.

7. Katzoff, S., and Hannah, Margery E.: Calculation of Tunnel-Induced
   Upwash Velocities for Swept and Yawed Wings. NACA TN 1748, 1948.

8. Theodorsen, Theodore: The Theory of Wind-Tunnel Wall Interference.
   NACA Rep. 410, 1931.

9. Glauert, H.: Wind Tunnel Interference on Wings, Bodies and Airscrews.
   R. & M. No. 1566, British A.R.C., 1933.
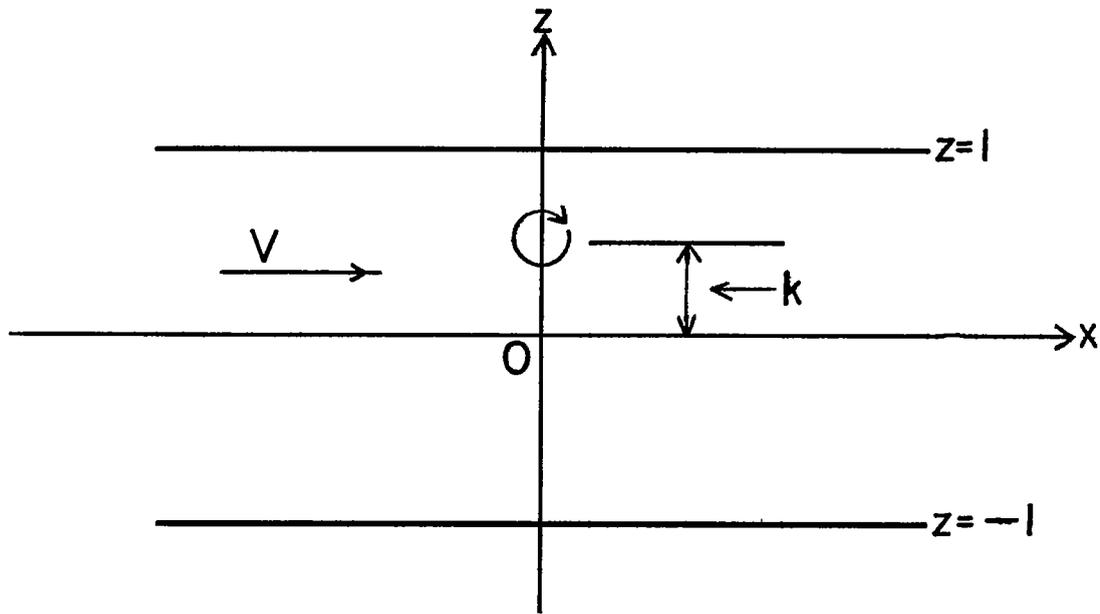
Figure 1.- Sketch showing two-dimensional slotted tunnel of unit semi-height, coordinate axes, and vortex location.
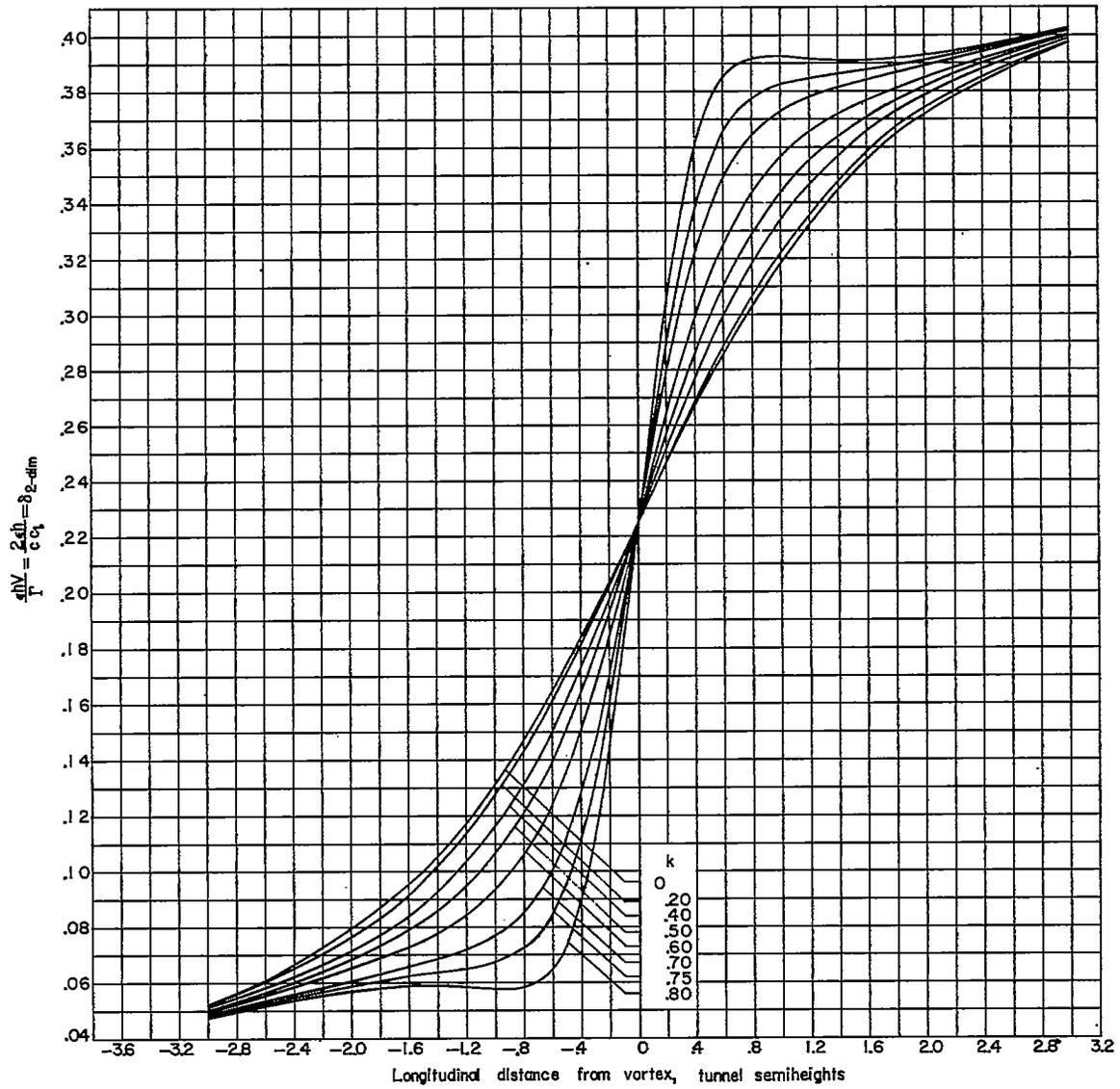
(a) $\dfrac{1}{g+1} = 0.9.$

Figure 2.- Longitudinal distribution of tunnel-induced downwash angle
for a lifting vortex in a two-dimensional slotted tunnel.
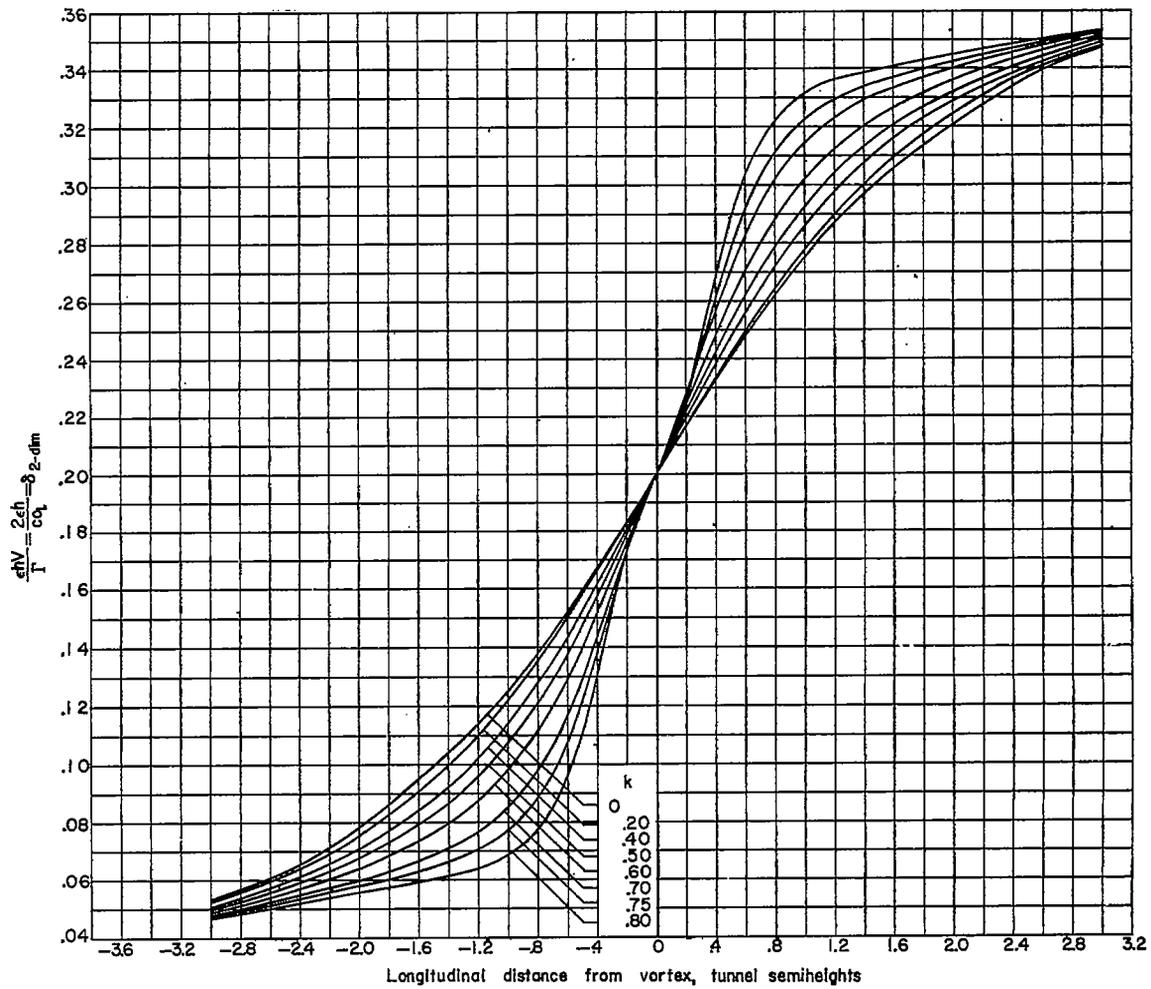
(b) $\dfrac{1}{g + 1} = 0.8.$

Figure 2.- Continued.
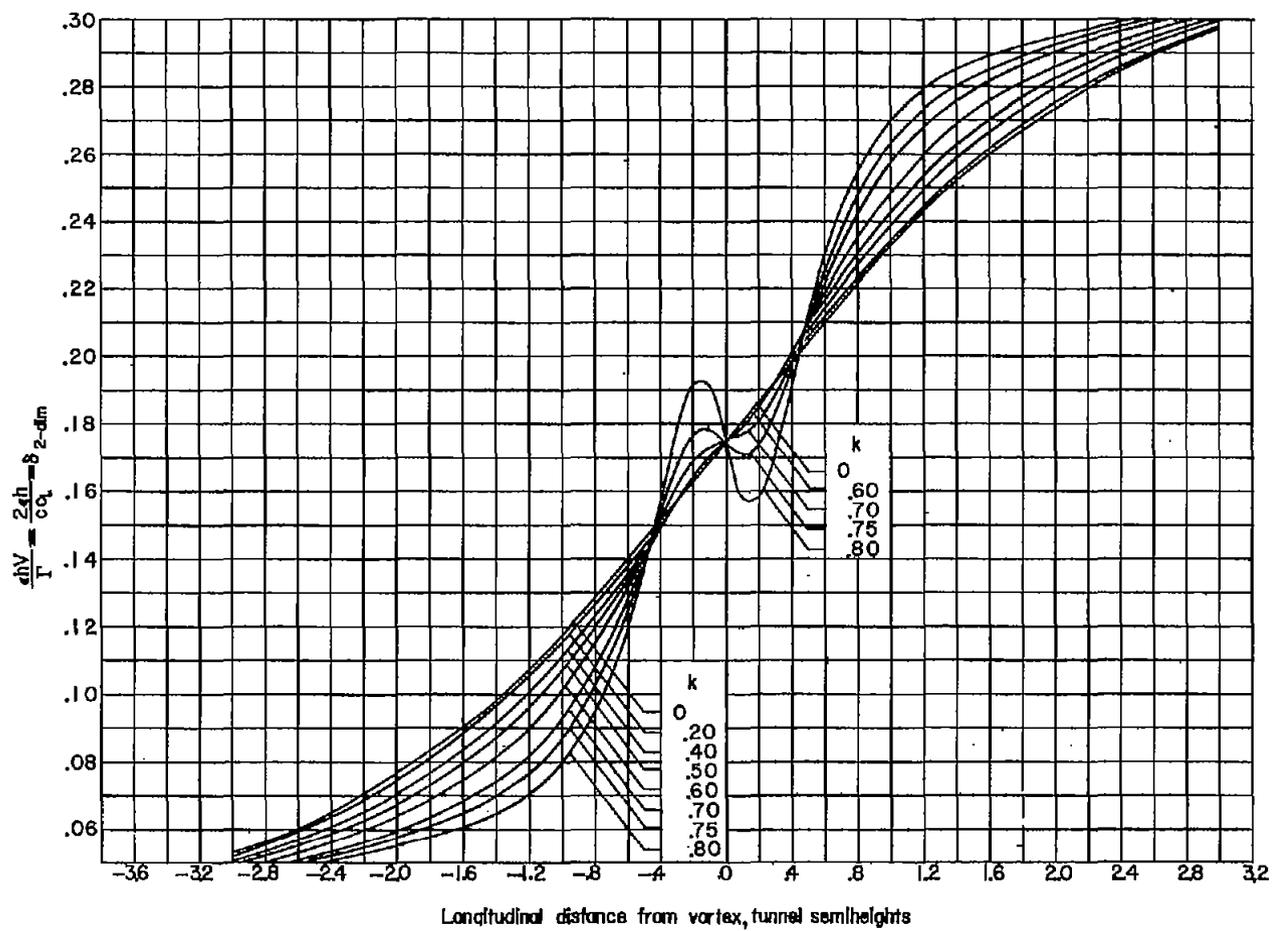
(c) $\dfrac{1}{g + 1} = 0.7.$

Figure 2.- Continued.
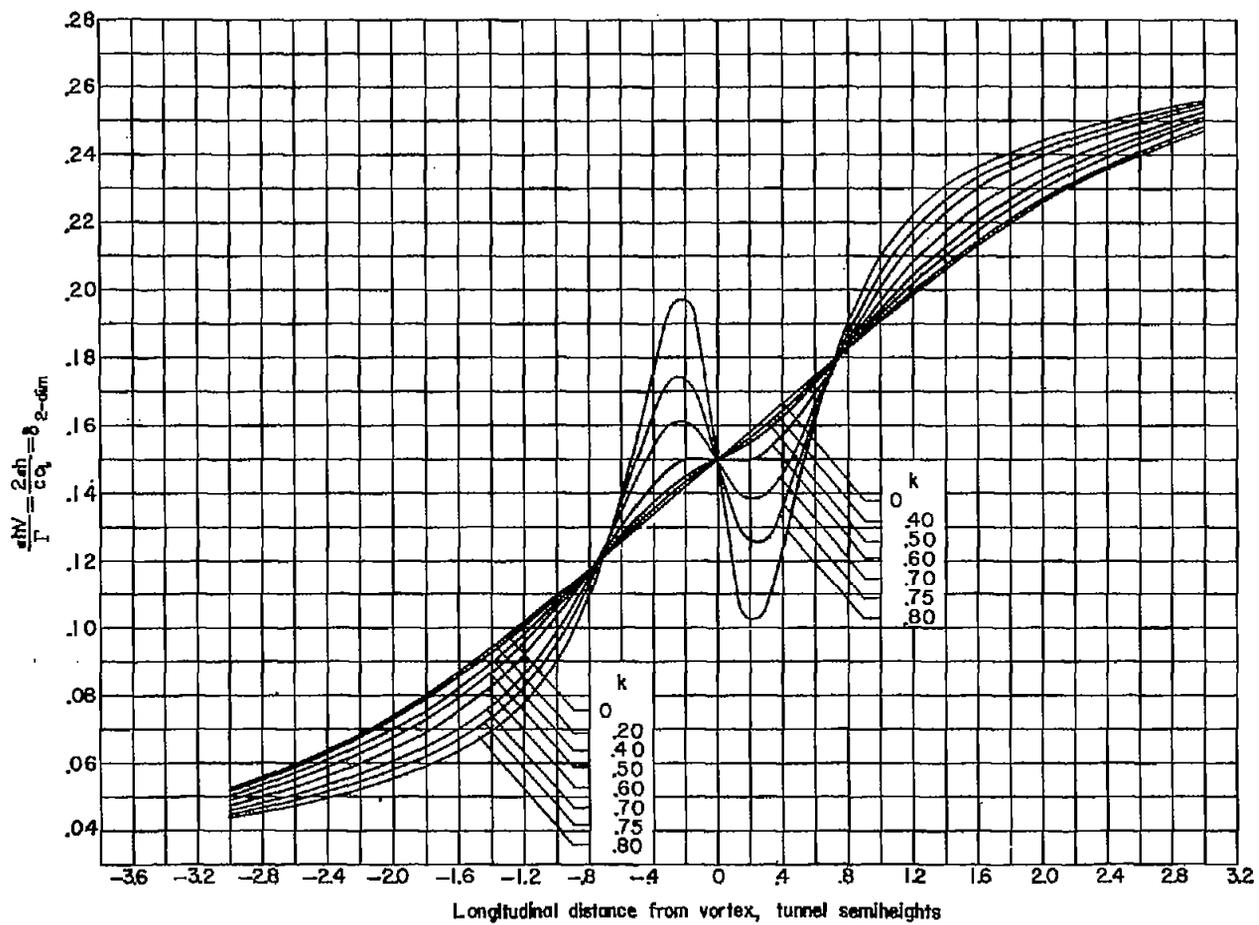
(d) $\dfrac{1}{g+1} = 0.6.$

Figure 2.- Continued.
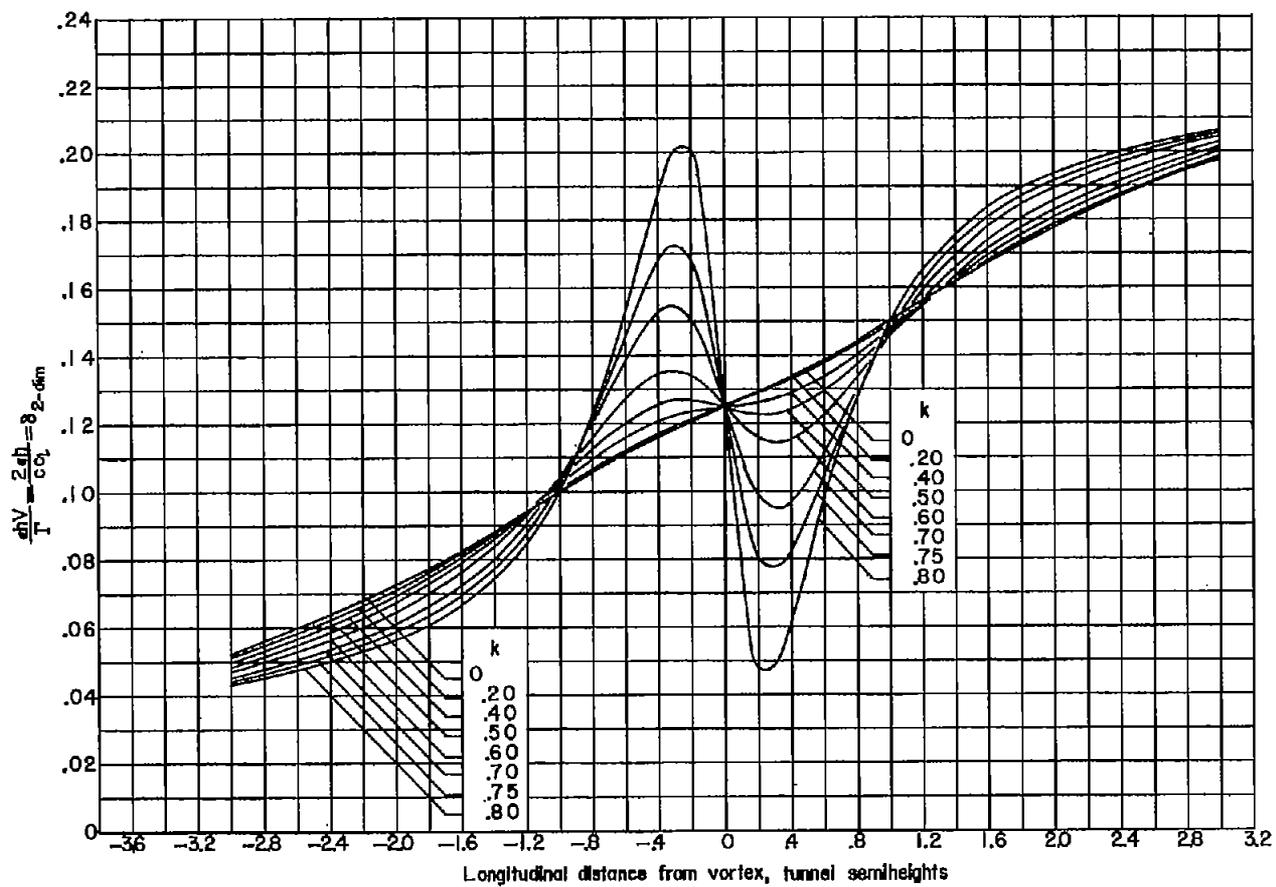
(e) $\dfrac{1}{g+1} = 0.5.$

Figure 2.- Continued.
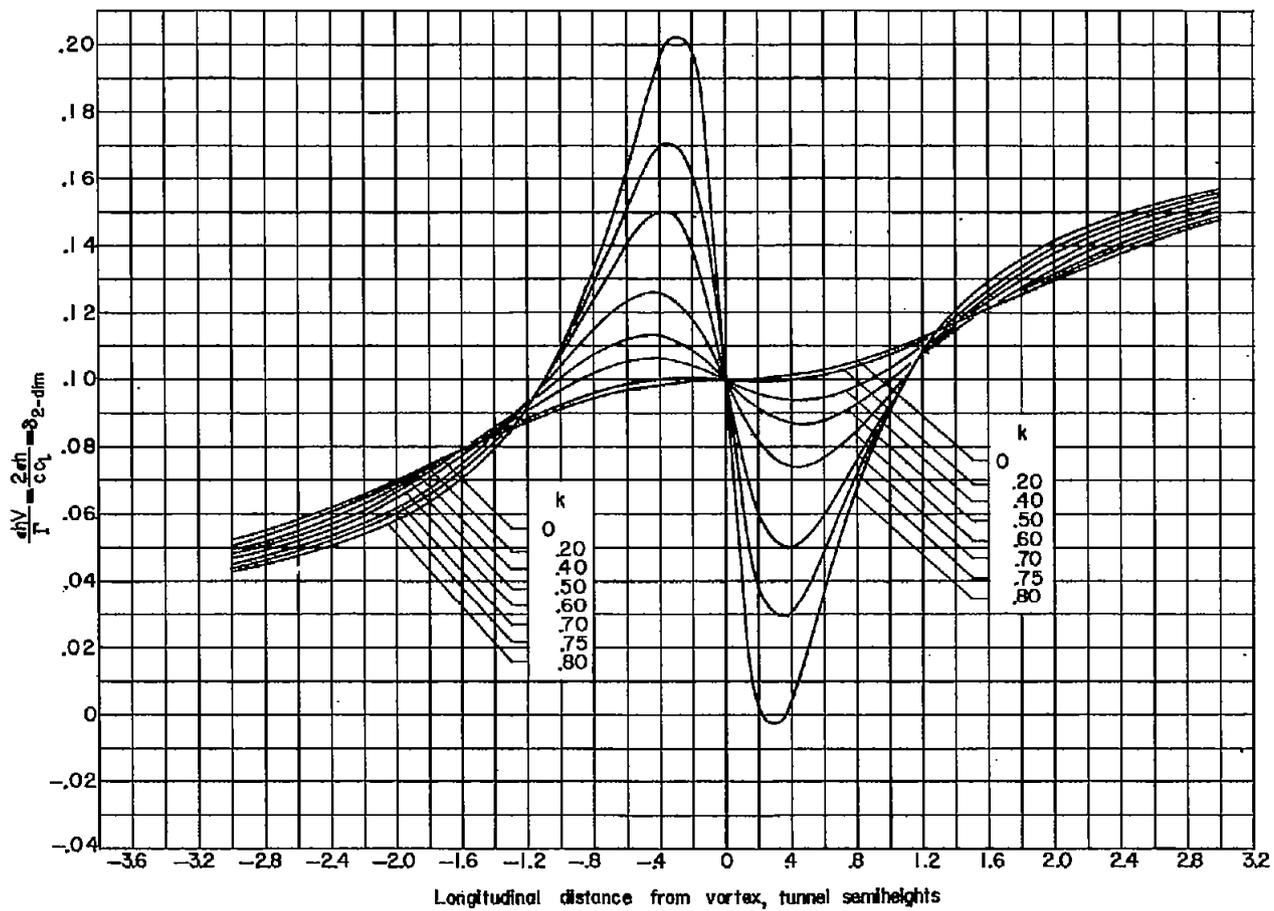
(f) $\dfrac{1}{g+1} = 0.4.$

Figure 2.- Continued.
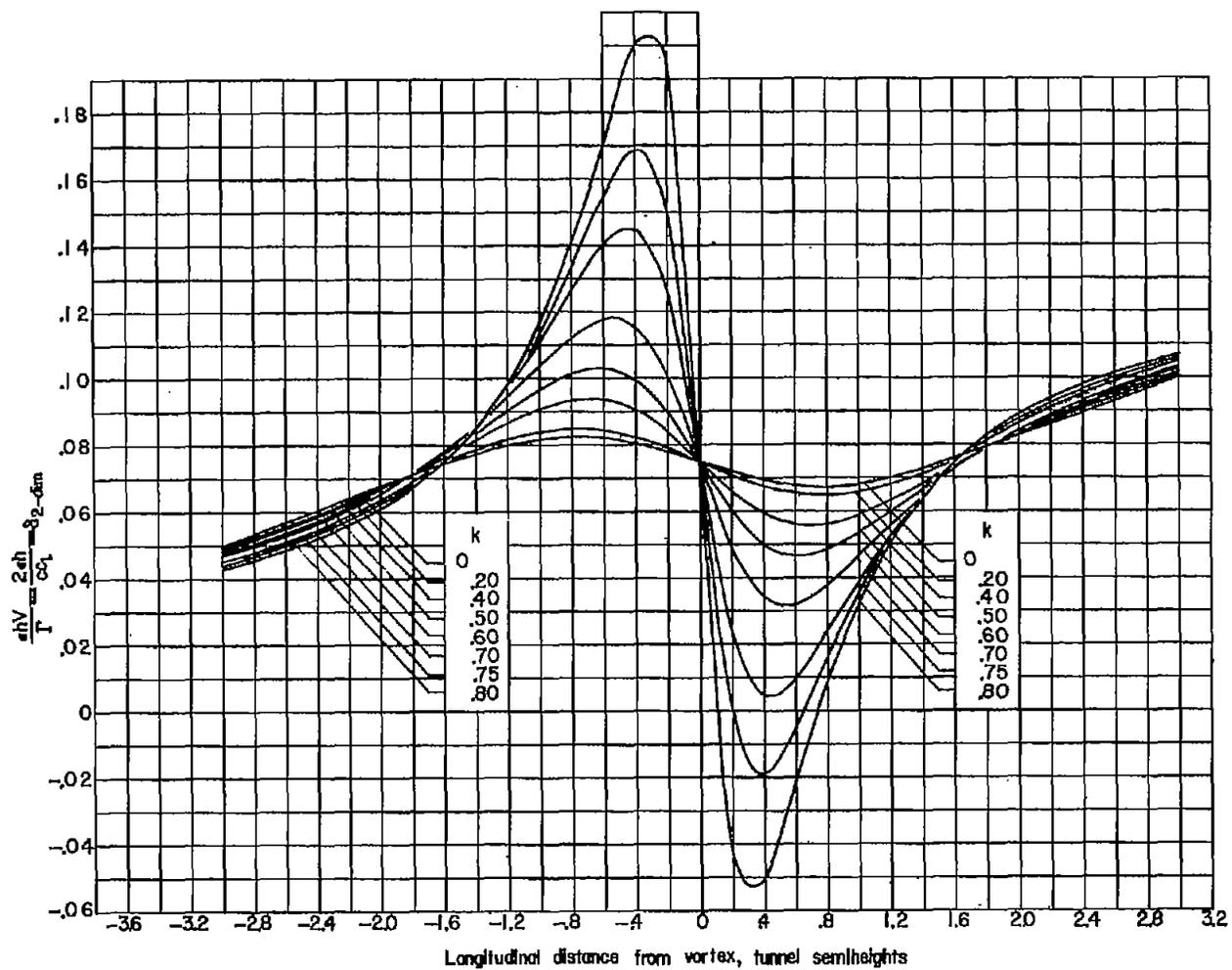
(g) $\dfrac{1}{g+1} = 0.3.$

Figure 2.- Continued.
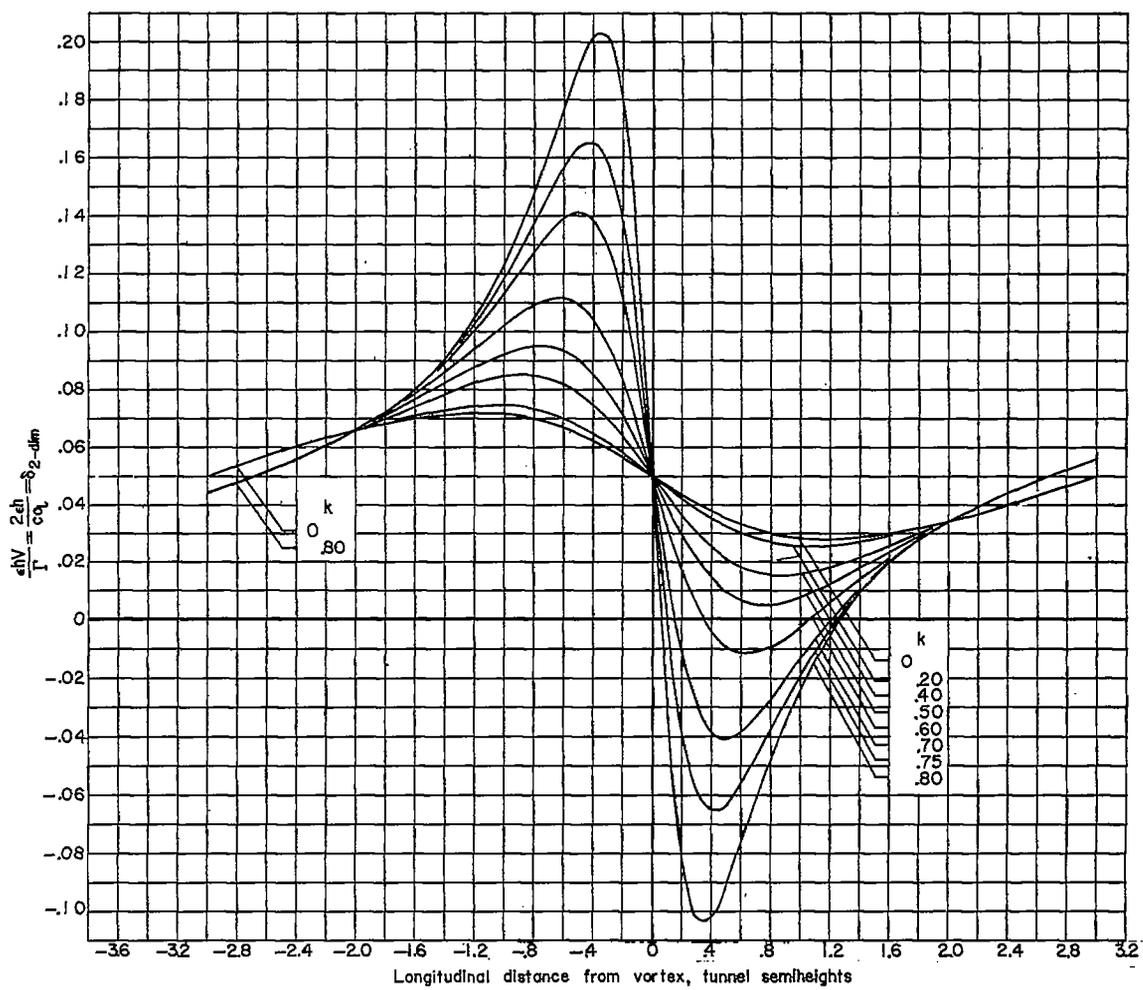
(h) $\dfrac{1}{g + 1} = 0.2.$

Figure 2.- Continued.
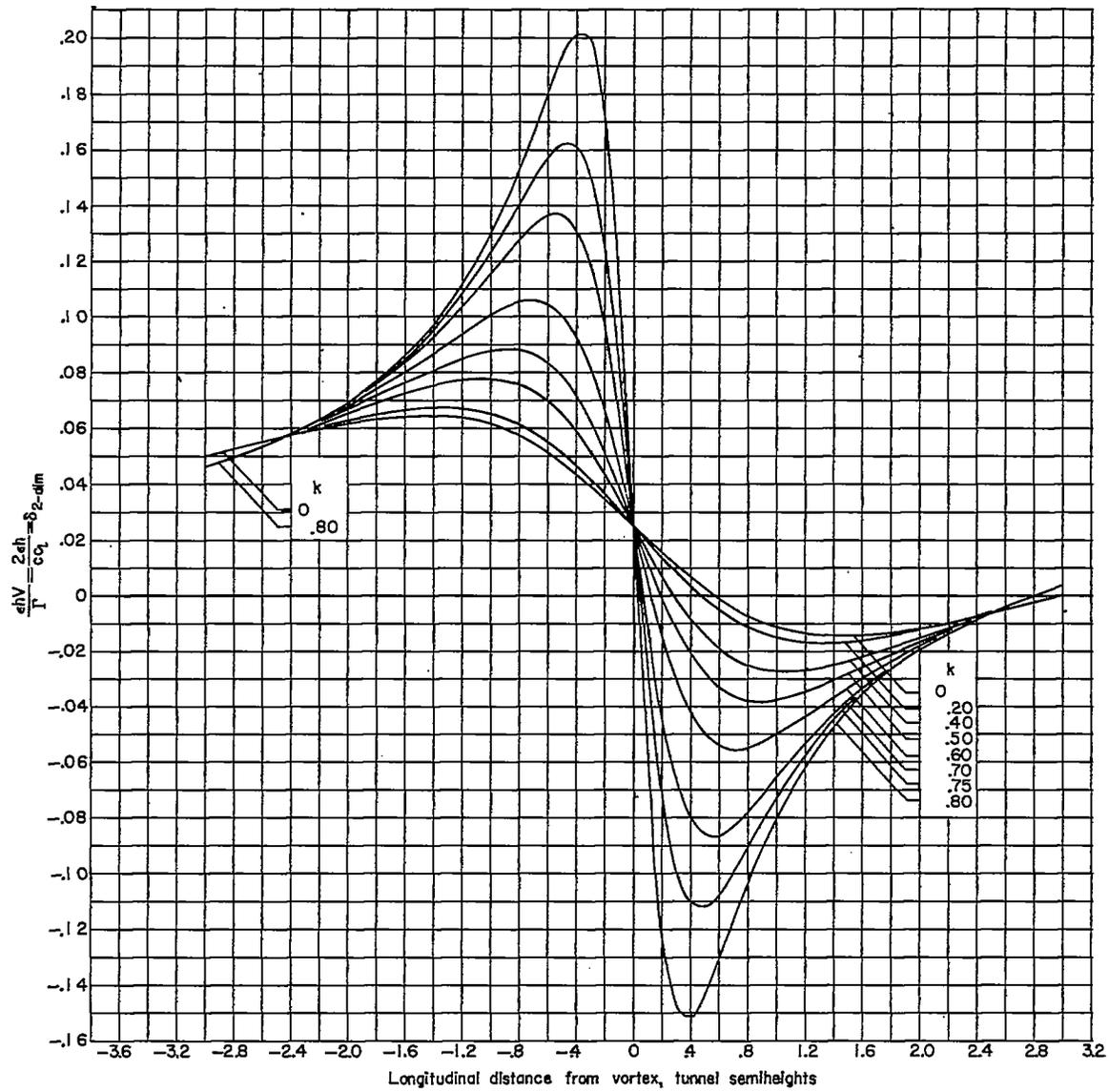
(i) $\dfrac{1}{g + 1} = 0.1.$

Figure 2.- Concluded.
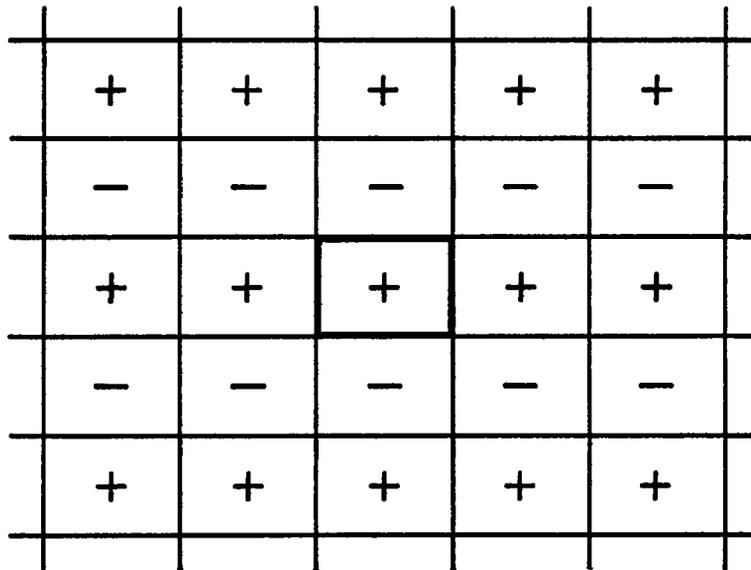
(a) Exact image system.
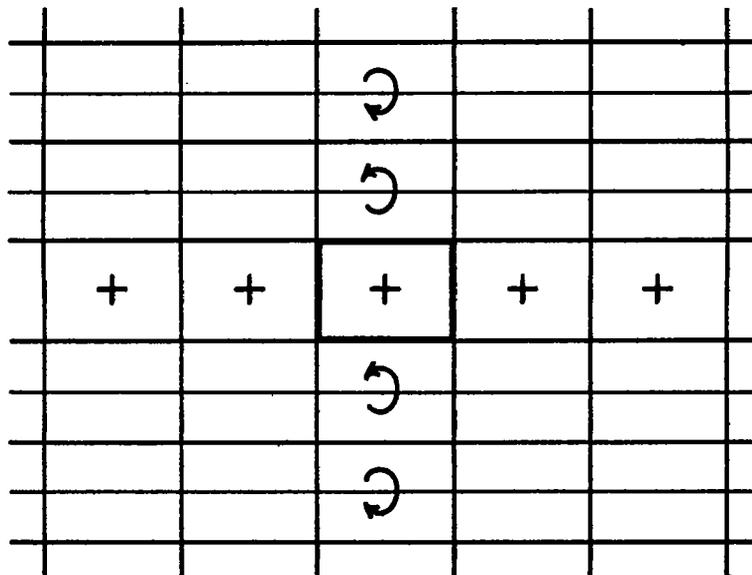
(b) Approximate image system. Doublet lines above and below the center
     have been replaced by horseshoe vortices of span equal to the tun-
     nel width.

Figure 3.- Image systems for a doublet line in a closed
                    rectangular tunnel.
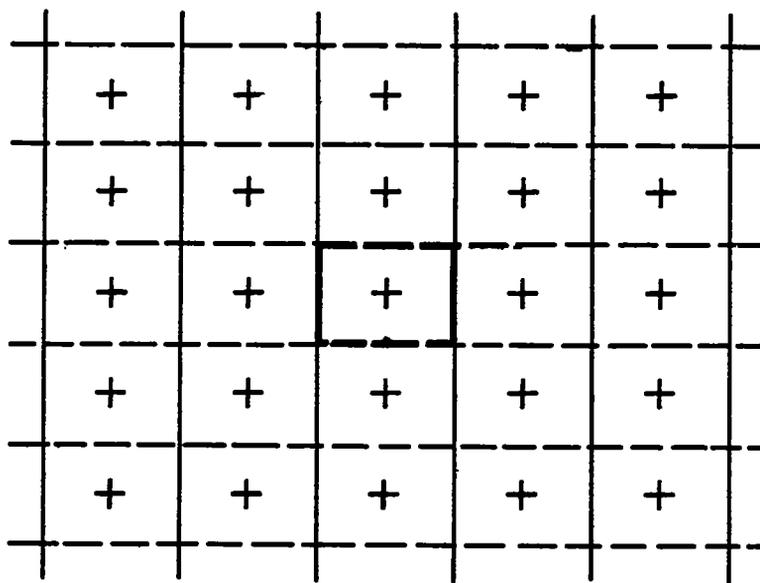
(a) Exact image system.
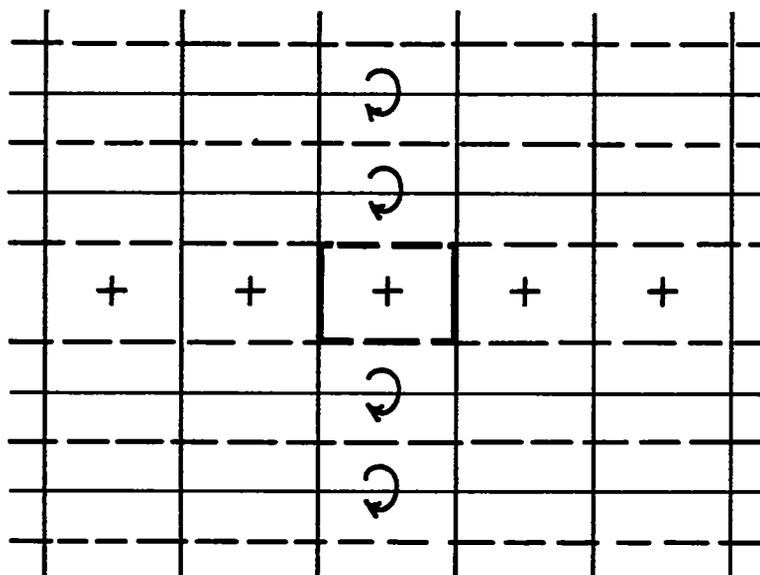
(b) Approximate image system. Doublet lines above and below the center
    have been replaced by horseshoe vortices of span equal to the tun-
    nel width.

Figure 4.- Image systems for a doublet line in a rectangular tunnel with
            closed side walls and open top and bottom.
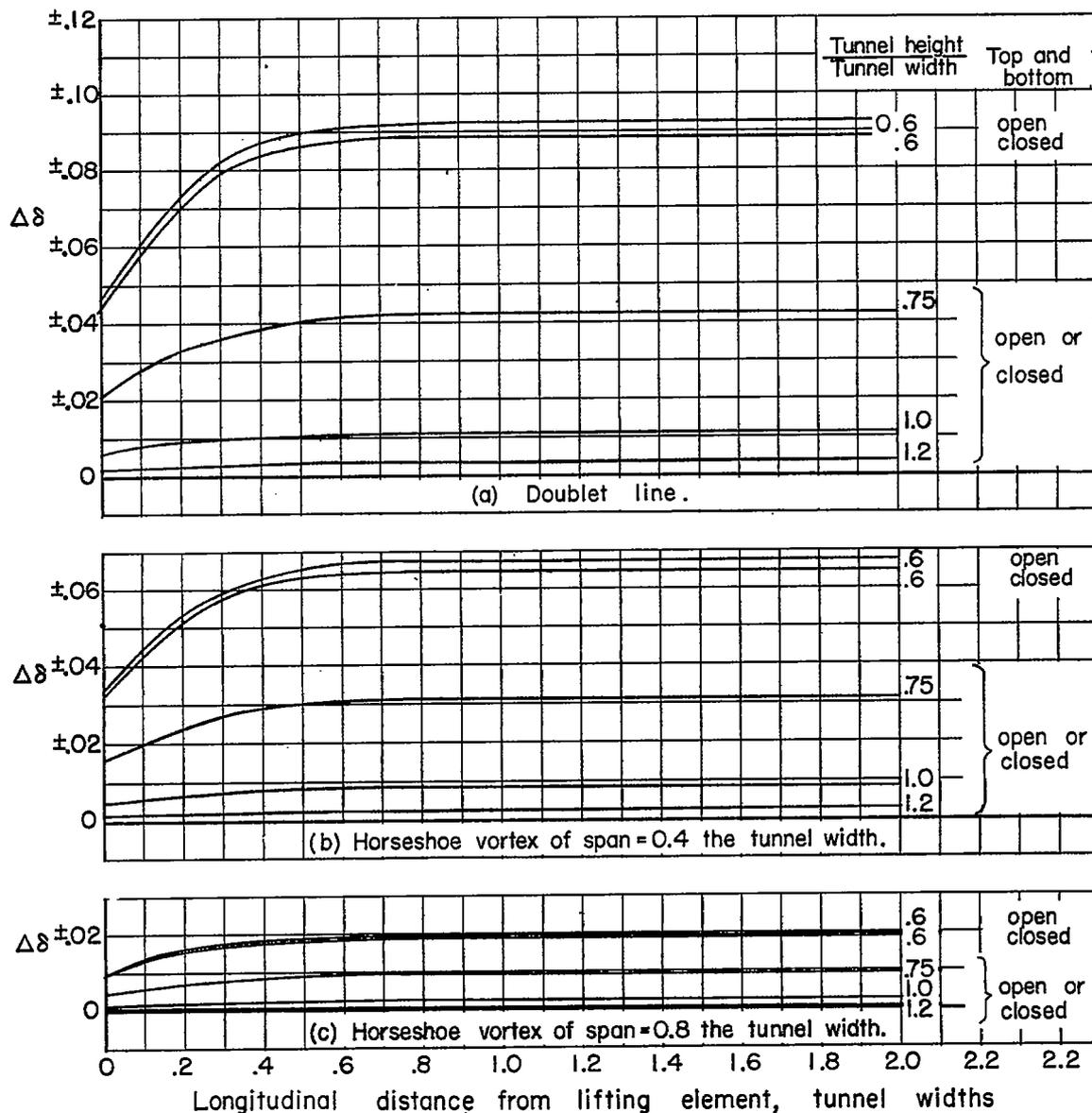
Figure 5.- Plots of $\Delta\delta$ (correction factor given by the exact image
system of fig. 3(a) or 4(a) minus correction factor given by the
approximate image system of fig. 3(b) or 4(b)). Positive values are
for the tunnel with open top and bottom, and negative values are for
the closed tunnel.
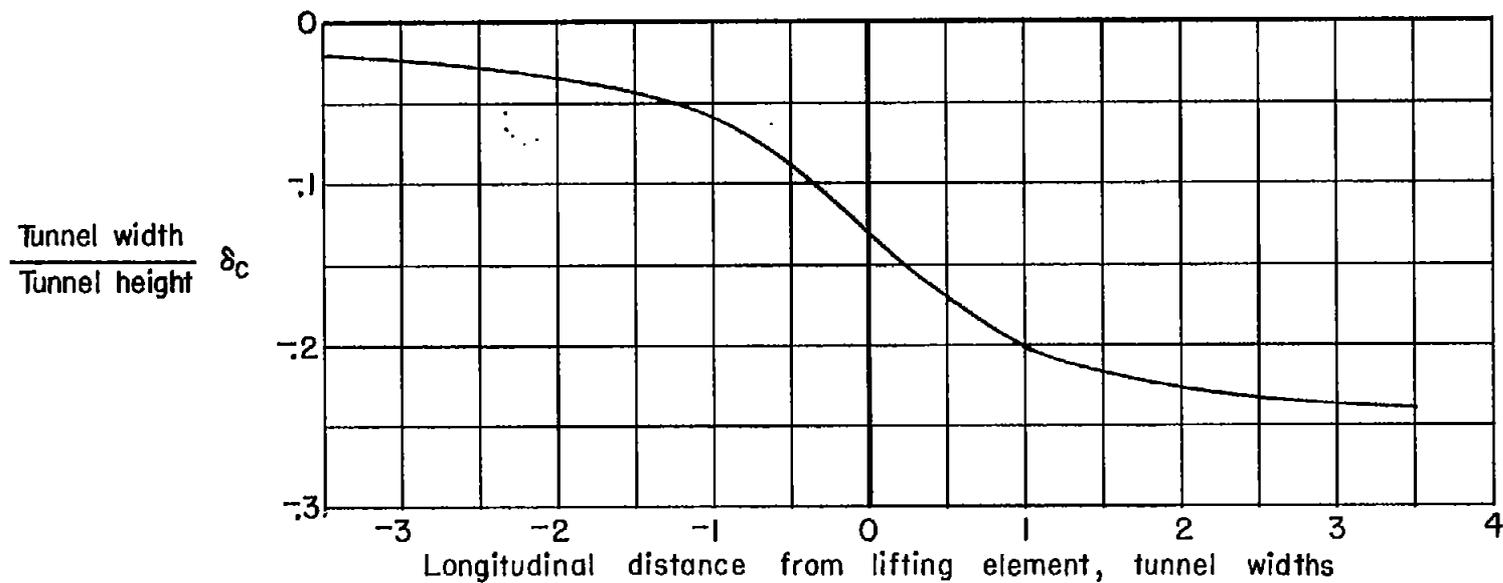
Figure 6.- Contribution δ_c of the center row of doublet images to the tunnel correction factor.
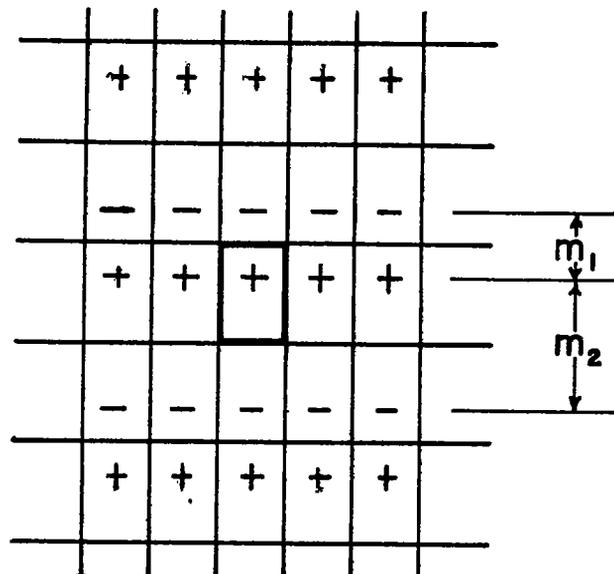
(a) Exact image system.
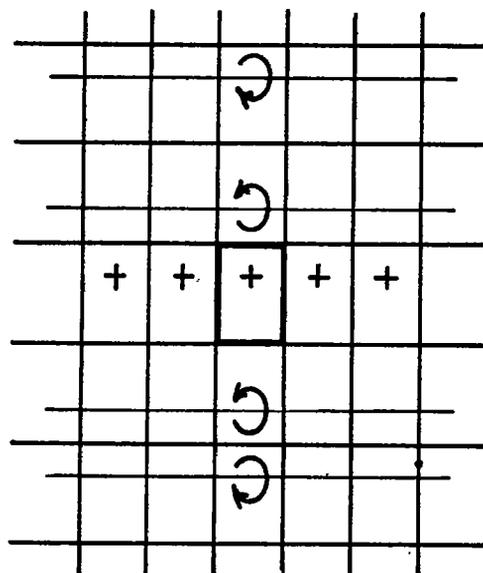
(b) Approximate image system. Doublet lines above and below the center
      have been replaced by horseshoe vortices of span equal to the tun-
      nel width.

Figure 7.- Image systems for a doublet line above the center of a closed
                              rectangular tunnel.
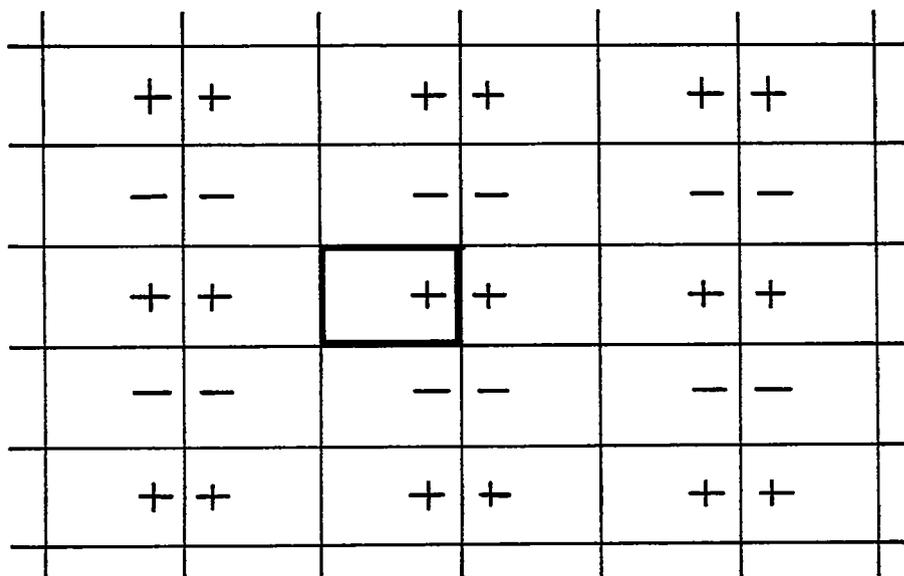
(a) Doublet near the side wall.
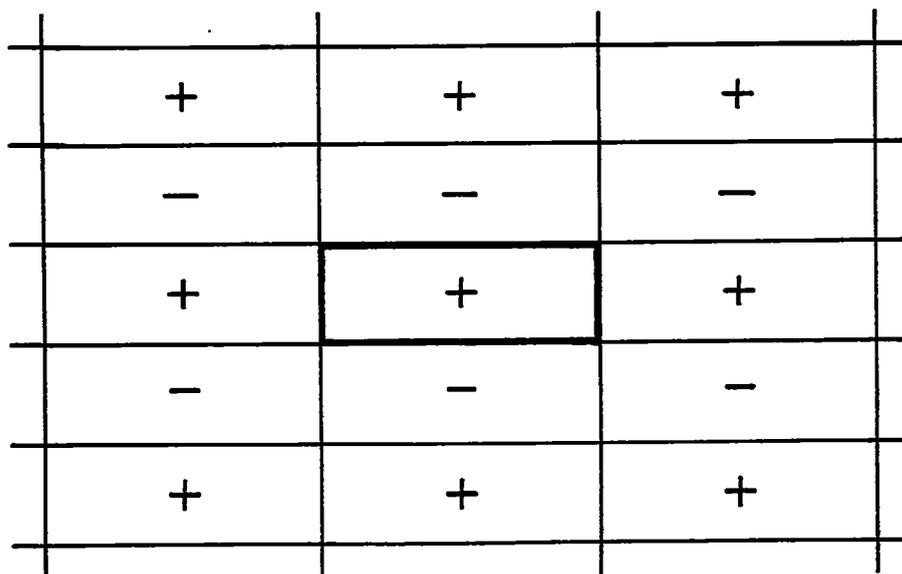
(b) Doublet at center of a tunnel having twice the width of the tunnel
diagrammed above.

Figure 8.- Image system for a doublet near the side wall of a closed
rectangular tunnel, and comparable image system for a doublet at the
center of a tunnel twice as wide as the first.